Effect of cuting parameters on the generated surface integrity of hard-turned martensitic AISI 52100 bearing steel

Available online at www.sciencedirect.com

ScienceDirect

Procedia CIRP 115 (2022) 154–159

www.elsevier.com/locate/procedia

10th CIRP Global Web Conference – Material Aspects of Manufacturing Processes

Effect of cutting parameters on the generated surface integrity of hard-turned martensitic AISI 52100 bearing steel

Sahith Kokkirala[a,*], Jonas Holmberg[b], Uta Klement[a], Roger Lundstrom[c], Hirotsugu Iwasaki[d], Seyed B. Hosseini[a,b]

[a]*Chalmers University of Technology, Division of Materials and Manufacturing, Hörsalsvägen 7B, Gothenburg, Sweden*
[b]*RISE AB, Department of Manufacturing Processes, Argongatan 30, Mölndal, Sweden*
[c]*AB SKF, SE-41550 Gothenburg, Sweden*
[d]*SUMITOMO ELECTRIC Hartmetall GmbH, Konrad-Zuse-Str. 9, 47877 Willich, Germany*

* Corresponding author. Tel.: +46 734959063. *E-mail address:* sahithk@chalmers.se

Abstract

Hard turning offers improved manufacturing efficiency but requires great control of the cutting process to achieve the required machining-induced surface integrity with respect to residual stresses, surface topography, and near-surface microstructure. This research work is focused on studying the effect of the cutting speed, feed rate, depth of cut, chamfer angle, and coolant pressure on the surface integrity after hard turning of martensitic AISI 52100 steel. The results showed that the feed rate had a significant influence on the residual stresses and the surface topography. The discontinuous mechanically induced white layer was observed at high cutting speed and high chamfer angle with increased thickness.

Keywords: Hard turning; surface integrity; residual stress; white layer; surface topography

1. Introduction

The surface integrity of the machined components is often the major concern for the manufacturing industry as it affects the component fatigue performance [1]. The machined parts are often subjected to variable and cyclic loads and hence the surface integrity plays an important role to reduce the risk of premature failure [2]. Experimentally observed, the fatigue behavior is influenced by the surface roughness and residual stresses [2]. The surface integrity depends on the finishing process as it alters the residual stresses, surface roughness, and microstructure. The hard turning process has gained interest over the last few decades compared to the grinding operation as it offers a cost-efficient and environmentally friendly process with the possibility of roughing and finishing in one setting and thus in a shorter processing time [3,4]. The process is performed with geometrically well-defined cutting tools on materials with higher hardness (> 45 HRC) to generate the required surface integrity [1,3]. Depth of cut, feed rate, cutting speed, tool chamfer angle, tool nose radius, and coolant pressure during the machining operation are the main cutting parameters in hard turning which have a significant effect on the generated surface integrity [1]. AISI 52100 is a high carbon chromium steel with favorable functional performances due to its high hardness and mechanical strength resulting in high wear resistance properties [1,3]. By varying the cutting parameters during the hard turning process on AISI 52100 steel, it is possible to alter the surface integrity to achieve favorable residual stress profiles, surface

10.1016/j.procir.2022.10.066

topography, and microstructural behavior [2]. Therefore, a thorough understanding and careful control of these parameters in generating the surface integrity of AISI 52100 is necessary and needs to be studied.

The effect of cutting-edge geometry on the residual stress is studied by Thiele et al [5] and concluded that the increased edge hone radius generates high compressive stresses on the finish hard turned AISI 52100 steel. Several tests conducted by Capello et al. [7] on hard-turned samples concluded that feed rate and tool nose radius have a significant impact on residual stress generation. A similar effect of feed rate and cutting speed on compressive residual stresses are observed by Jomaa et al. [8] on AISI 4340 induction hardened steel. Revel et al. [9] concluded that higher cutting speeds result in better subsurface compressive residual stresses.

However, there is a limited study of cutting parameters and tool geometry effects on surface roughness. Zhang et al. [10] stated the increase in chamfer angle and width has a reduced surface roughness generation but increased tool wear. From several investigations, it is concluded that surface roughness (Ra) is significantly affected by the feed rate parameter and the tool nose radius [11,12].

It is well known that under certain machining conditions, the hard turning process can generate white and dark layers on the surface. The layers are distinguished under the light optical microscope when etched as first observed by Stead [13] on the surface of steel wire ropes in 1912. Hosseini and Klement [14] studied the formation of white layers in the hard-turned AISI 52100 steel and distinguished the thermal and mechanical induced white layers depending on the pressure and temperature effects during the machining. There are several controversial effects of white layers on fatigue life due to their residual stress distribution and underlying dark layer effects if formed.

As reported by Hosseini et al. [14] due to its nano-sized grains and elongated carbide structure in the microstructure, which is created through dynamic recovery, mechanically induced white layers had a hardness ~26% higher than the bulk hardness with reduced retained austenite content and high sub-surface compressive stresses. The thermally induced white layer consists dark layer beneath with being ~14% softer than the bulk material and generated tensile residual stresses on the surface white layer due to the phase transformation effects. It was concluded that the lack of a dark layer in mechanically induced white layers shows a possibility of ultra-high strength machined surface which can be utilized for the applications needed for superior mechanical and wear properties.

From the above literature review, the clear understanding of the varying feed rates, varying cutting speeds, and varying depth of cut for 2 mm tool nose radius on the surface integrity is not well understood in generating the low surface roughness profile, high subsurface compressive residual stresses and mechanically induced white layer from the fresh cutting insert. The aim of this paper is to investigate these effects in relation to the surface and subsurface residual stresses, surface topography, and microstructure.

2. Materials and Methods

2.1. Workpiece material

AISI 52100 chromium-containing high carbon steel grade is used for the study and the chemical composition of the material is given in Table 1. The material is widely used in bearing applications. The final heat-treated samples consist of martensitic or bainitic microstructure with less than 2% by volume of retained austenite. The hardness of the sample is ~ 61 HRC in each case.

Table 1. AISI 52100 steel chemical composition (wt.%) [3]

Fe	C	Mn	Si	Cr	S	P
Bal.	0.95	0.32	0.26	1.42	0.001	0.009

2.2. Hard turning

The turning tests were performed on a MONFORTS RNC500 SingleTurn machine and coated BNC 2125 inserts (DNGA 1506 S01015/S01035) with a 2mm nose radius were used as cutting tools throughout all tests. For each design of the experiment, a fresh cutting insert was used. The turning tests were done on the cylindrical ring with a length of 60 mm and an outer diameter of 180 mm. The required dimension is selected based on the real-time industrial application. During the tests, the conditions for cutting speed (V_c), feed rate (f), depth of cut (a_p), coolant pressure (P), and tool chamfer angle (γ) were varied. Table 2 provides the factors and factor levels that were considered to generate the design of experiments. In total, 32 hard turning tests were generated with 5-factor levels.

Table 2. Design of experiments (DOE) variables.

Factors	V_c (m/min)	f (mm/rev)	a_p (mm)	P (bar)	γ (°)
Low	60	0.05	0.05	20	15
High	110	0.2	0.2	150	35

In figure 1, the test is illustrated. On each ring, 2 tests were performed which in total resulted in 16 rings that were created in this study. First, the length of 60 mm in combination with f = 0.2 mm was machined, followed by machining 25 mm with f = 0.05 mm. Before sectioning the rings, both the residual stresses and the surface topography were measured. Then the rings were cut into smaller sections to perform the microstructural analysis for all the 32 unique surfaces.

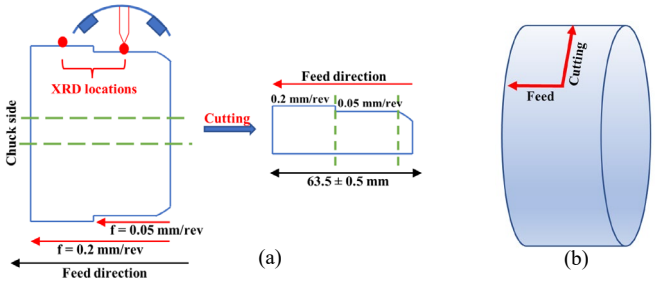

Fig. 1. a) Representation of the sample ring machined with varying feeds. b) Cutting and feed direction for XRD measurements

2.3. Characterization techniques

The residual stresses were measured using the X-ray diffraction technique. The XSTRESS 3000 G2R X-ray diffractometer from Stresstech with Cr-Kα source and 2 mm collimator was used to measure the residual stresses along the feed and cutting direction as illustrated in Fig. 1. Two position-sensitive detectors (PSD) are used at 156.4° diffraction angle on the arc-shaped detector holder to measure BCC/BCT [211] interplanar lattice spacing. The modified $\sin^2(\Psi)$ method was used with tilt angles from -45° to + 45° to measure the lattice spacing and eventually determine the residual stresses using Xtronic software. The depth profiles for residual stress evaluations were measured from the surface down to 100 µm with a total of 6 measuring points (0, 5, 10, 20, 50, and 100 µm). The material was removed using the electropolishing technique with saturated salt electrolyte and the depth measurement was performed using a dial gauge.

The surface topography measurements were done along the surface at 3 different locations on the rings and the results are averaged. The Sensofar 3D optical profiler with VSI (vertical scanning interferometry) technique is used to measure the surface roughness of the hard-turned rings. Three measurements were performed around the ring over and 7.4x1.3 mm stitched area with a lateral resolution of 1.29 µm. The measured surface data was processed by form removal using a 2nd order polynomial followed by a filter using a spatial median noise-reduction algorithm with a window size of 5x5 points. The arithmetic mean deviation of the roughness profile, Ra, was calculated in accordance with ISO 4287.

The sample was cut and hot-mounted in a 40 mm diameter polyfast bakelite. The polishing steps are carried out until the 1 µm diamond suspension is used to create a scratch-free surface. The samples were etched with 2% nital solution to investigate the machined surface microstructure. A Zeiss Axioscope 7 light optical microscope was used to study the hard-turned microstructure. For investigation of the nano-sized microstructure of the white layer on the surface, a Zeiss Gemini 450 scanning electron microscope was used.

3. Results and Discussions

3.1. Effect of cutting parameters on residual stress

Fig. 2 shows the surface residual stresses of varying cutting parameters. As can be seen, the maximum compressive residual stresses are observed for low f (0.05 mm/ rev) in all the cases. With low P and high γ as shown in Fig. 2b, high compressive stresses are observed at a_p 0.2 mm for the 60 m/min and 110 m/min.

The maximum surface residual stress is observed in Fig. 2d along the feed direction at low f (0.05 mm/rev), low a_p (0.05 mm), and low V_c and at high P (150 bar) when using larger γ (35°) with a value of -927.3 MPa. For the low P (20 bar), the maximum surface residual stress is observed in Fig. 2b at a low f, high a_p, and high γ for both the low and high cutting speeds being around -725.3 MPa. Due to the low coolant pressure, high thermal effects due to the rise in temperature are observed resulting in low compressive stresses compared to the 150 bar coolant pressure. As previously shown by Dahlman et al. [16] for both coolant pressures, a tool with a higher chamfer angle, due to its larger contact area, created high surface compressive residual stresses resulting in high mechanical stresses compared to the lower chamfer angle.

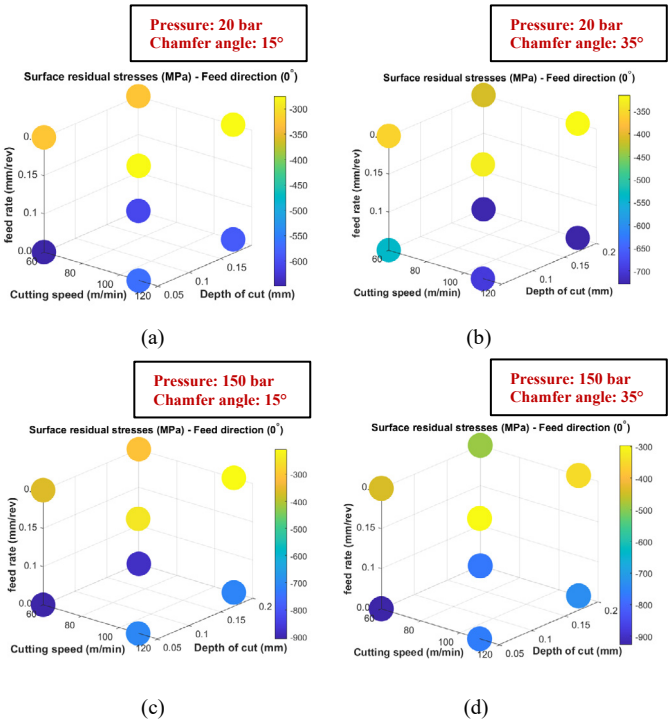

Fig.2. Surface residual stresses along the feed direction with varying pressure and chamfer angle.

The surface residual stresses along the cutting direction are illustrated in Fig. 3. The trend along the cutting direction is different compared to the feed direction. High compressive residual stresses are generated at higher f (0.2 mm/rev) and low V_c (60 m/min). The depth of cut has no significant influence in this direction. The observation of the effect of depth of cut results is in line with the results observed by Philippe et al. [15]. The maximum compressive stresses generated on the surface are lower than the compressive stresses along the feed direction. The effect of high temperature and high cutting forces are observed in the cutting direction which results in lower surface compressive stresses. At low f, low V_c, and high a_p, surface tensile stresses are generated for the samples with low coolant pressure of 20 bar as observed in Fig. 4a and 4b.

The effect of the varying cutting parameters on the generated subsurface residual stresses is illustrated in Fig. 4 and Fig. 5. Each figure has 4 subfigures (a, b, c, and d) representing the low feed rate and high feed rate effects for varying pressure and chamfer angle. The residual stresses along the feed direction for the low feed rate (0.05 mm/rev) in Fig. 4a, 4c, 5a, and 5c do not have a regular hook-shaped residual stress profile as observed for hard-turned samples. Instead, a different profile is observed, resembling that of a ground sample profile with high compressive stresses generated at the surface rather than the sub-surface.

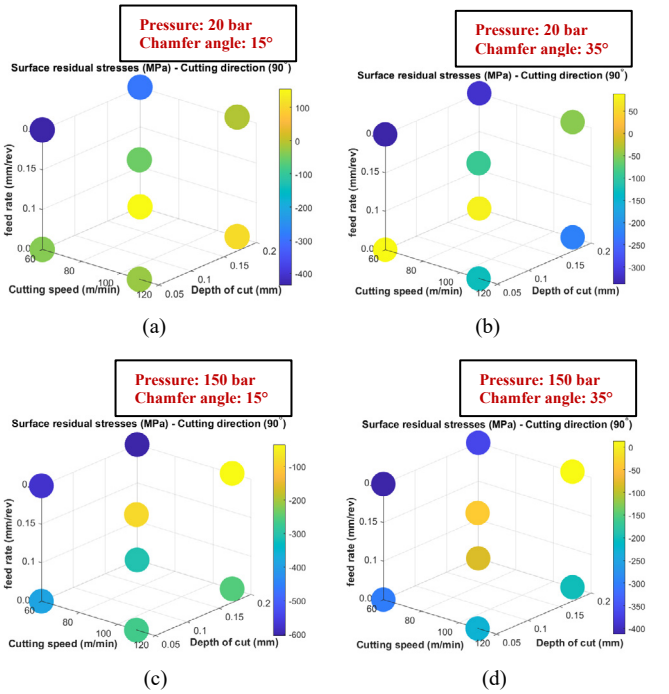

Fig.3. Surface residual stresses along the cutting direction with varying pressure and chamfer angle.

Fig. 4a and Fig. 4b represent the residual stress depth profile for the low P and low γ parameters. The high feed rate, as shown in Fig. 4b, creates high subsurface compressive residual stresses at a depth of between 5 µm – 10 µm.

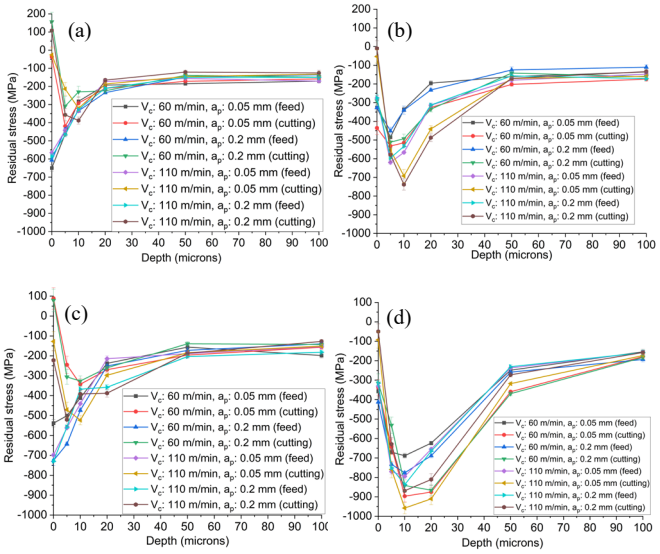

Fig.4. Residual stresses measured at a) low f (0.05 mm/rev) b) high f (0.2 mm/rev) for low P=20 bar and low γ=15° c) low f (0.05 mm/rev) d) high f (0.2 mm/rev) for low P=20 bar and high γ=35°.

Along the cutting direction, when using 110 m/min cutting speed, the surface stresses show low compressive stresses at both the low and high a_p parameters most likely connected to the increase in temperature with increasing cutting speeds. Keeping the pressure constant at 20 bar and increasing the chamfer angle to 35°, the hard turning process affects the shallow nature of the subsurface compressive stresses to a depth of 50 µm in samples with high feed rates, as in Fig. 4d. The compressive stresses also shift to a greater depth of around 10 - 20 µm. With increasing chamfer angle for low f (0.05 mm/rev) and low P (20 bar), a small variation in the residual stress depth profile is observed as seen in Fig. 4c when compared to Fig. 4a. But in the case of high f (0.2 mm/rev) and low P (20 bar) as seen in Fig. 4b and 4d, significant change in the residual stresses is observed with higher subsurface compressive stresses due to the increase in chamfer angle γ. With increasing feed rate and cutting speeds, higher compressive stresses are generated as observed by Wisley F. Sales et al. [2] The depth of cut has no significant impact on the residual stress generation compared to the cutting speed and feed rates [17]. The stresses along the cutting direction have higher compressive subsurface stresses than in the feed direction until a certain depth depending on the chamfer angle. This shows that the thermal influence along the cutting direction is insignificant in the subsurface region in comparison to the plastic deformation.

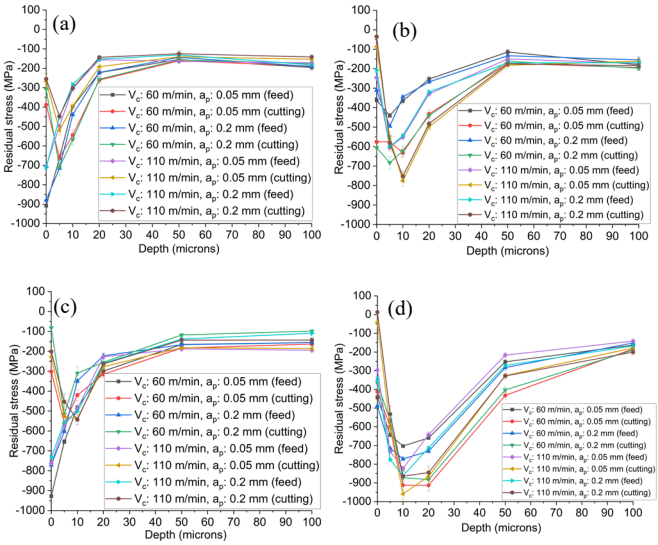

Fig.5. Residual stresses measured at a) low f (0.05 mm/rev) b) high f (0.2 mm/rev) for high P=150 bar and low γ=15° c) low f (0.05 mm/rev) d) high f (0.2 mm/rev) for high P=150 bar and high γ=35°.

Fig. 5a and 5b show the residual stress depth profile when using high P (150 bar) and low γ (15°). With increasing feed and increasing cutting speeds, a similar trend was observed i.e. higher compressive stresses are generated below the surface at about 5 - 10 µm. As shown in Fig. 5d, with increasing chamfer angle and at the high coolant pressure of 150 bar, a large displacement of compressive stresses into the subsurface, down to a depth of 20 µm, is observed, indicating greater mechanical effects with a high chamfer angle due to its large contact area with the workpiece Increasing cutting speeds reduces the surface compressive stresses due to the rise in temperature, but the subsurface has no obvious effect due to the coolant pressure along the cutting direction. A similar observation is reported by Bicek m et al. [21] while evaluating the residual stress profiles of the hardened machined samples under cryogenic and dry cutting conditions. This was also concluded by Hosseini et al. [19] when studying the cutting temperatures during the hard turning process.

For all the conditions above, the subsurface compressive residual stresses increase with the increased feed rate from 0.05 mm/rev to 0.2 mm/rev. This could be the consequence of the higher cutting forces generated due to the high feed rate which significantly increases the plastic deformation under the surface [16].

3.2. Effect of cutting parameters on surface roughness

The effect of cutting parameters on the surface roughness (R_a) is illustrated in Fig. 6. The lowest surface roughness of R_a 0.07 µm is generated with V_c = 110 m/min, a_p=0.05 mm, P=20 bar, γ=15° as seen in fig. 6a. The obtained R_a is the lowest surface roughness profile generated considering all the design of experiments. The effect of chamfer angle has no particular impact on the surface roughness profile. At a high feed rate, increasing cutting speed and depth of cut has no major effect on the surface roughness profile for high chamfer angle.

As observed in Fig. 7, a higher feed rate results in a ploughing effect indicating a stronger effect of feed rate on R_a. The roughness average is a function of nose radius and feed rate as shown by Grzesik [12]. Increasing the nose radius, and reducing the feed rate generates lower R_a. In addition to this, the increase in cutting speed from 60 m/min to 110 m/min lowers the average roughness profile which is also observed similarly by Philip et al. [15]. At the higher cutting speeds, the surface temperature increases and promotes the material softening phenomenon leading to the lower surface roughness average R_a. For the low feed rate of 0.05 mm/rev in Fig. 6a and 6c, the roughness average R_a for all the conditions is below 0.2 µm.

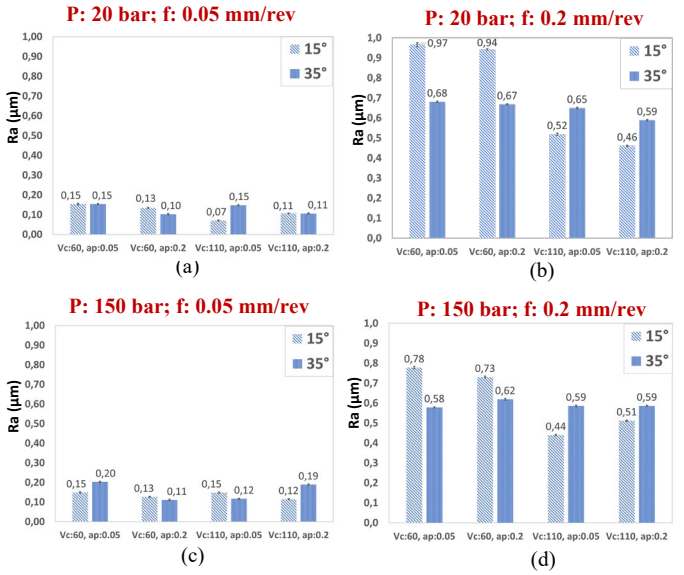

Fig.6. Surface roughness (Ra) measurements with varying parameters of cutting speed, depth of cut, feed rate, coolant pressure & chamfer angle.

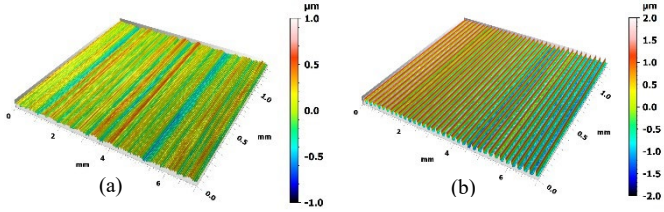

Fig.7. VSI generated surface roughness illustrating the major effect of feed rate a) 0.05 mm/rev b) 0.2 mm/rev for constant V_c = 60 m/min, a_p=0.05 mm, P=150 bar, γ=15°.

3.3. Effect of cutting parameters on microstructure

To understand the metallurgical behavior of all the machined samples, microscopic analysis was performed. All of the 32 samples were observed through a light optical microscope to correlate and evaluate the surface integrity. Even though the hard turning was performed by fresh tools on each sample, discontinuous white layer structures are generated on the machined surface with a thickness of less than 1 µm implying the generation of mechanically induced white layers [18]. Most of the discontinuous white layers are observed at the end of the feed grooves. As reported by Hosseini et al. [14] The discontinuous white layers are generated at the primary cutting-edge with the workpiece. The results are also in line with the observations made by Smith et al. [20] while examining the formation of white layers in AISI 52100 steel. By varying the cutting-edge geometry (tool wear and edge radius), the discontinuous white layer formation can be directed towards generating continuous white layers due to the contact duration, pressure, and temperature which are still to be investigated in this research. No dark layers are observed under the white layers, indicating that there were no major thermal effects. Fig. 8 illustrates the mechanically induced white layer generated at the machined surface. In Fig. 8c, nano-sized grain structures are observed with the M_3C carbides being plastically deformed along the feed direction indicating the predominant mechanical impact rather than thermal influence in generating the white layer which is stated by Hosseini et al. [3, 18] in their work on the white layer formation. Below the thin white layer region, the M_3C carbides are generally in spherical shape indicating no deformation.

Increasing the chamfer angle from 15° to 35° leads to an increase in white layer thickness to a few micrometers.

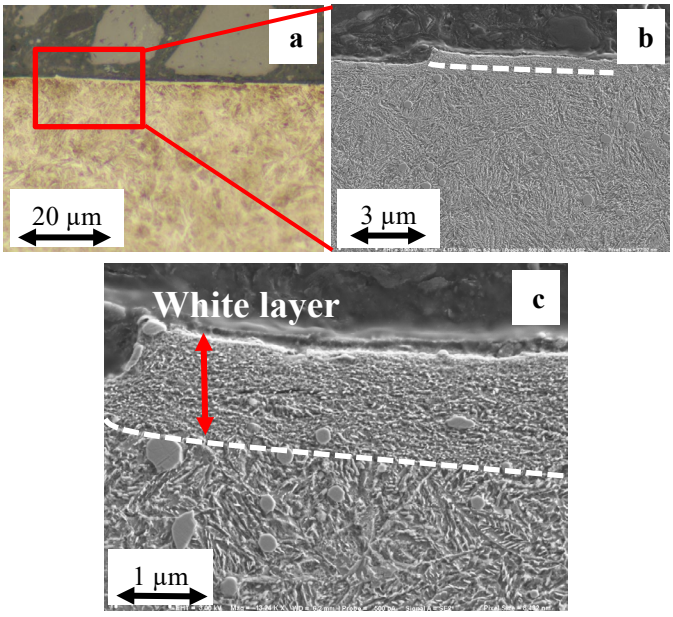

Fig.8. Mechanically induced white layer formed on the surface with fresh tool inserts with V_c=110 m/min, a_p=0.2 mm, f=0.2 mm/rev, P=150 bar & γ=35°. a) Light optical microscope image b) SEM image of OM c) Magnified image of mechanically induced white layer (< 1 µm) with nanocrystalline grains.

Regardless of the coolant pressure, the chamfer angle has a huge impact in generating the mechanically induced white layers due to its high contact pressure and resulting mechanical loads. Due to the thermo-mechanical loads, severe plastic deformation leading to dynamic recovery is generated in the machined surface resulting in a mechanically induced white layer [14].

4. Conclusions

This work investigates the effect of cutting parameters on the surface integrity after hard turning, which resulted in the following:

- Mechanically induced discontinuous white layers (< 1 μm) are observed in all the samples irrespective of the coolant pressure and chamfer angle. For high cutting speed and chamfer angle, the white layer thickness increases by a few hundred nanometers.
- Feed rate has a significant effect on both the residual stress profile as well as the surface topography. A high feed rate increases the subsurface compressive residual stresses, while a low feed rate generates a lower surface roughness.
- At the lowest feed rate, the residual stress profiles appeared to be comparable to residual stress profiles normally found after grinding.
- High feed rate generates higher subsurface compressive residual stresses and higher surface roughness. This can be compared to the low feed rate, which resulted in lower surface roughness and lower subsurface compressive stresses.
- High chamfer tool angle generates maximum compressive stress at a depth between 10 to 20 μm beneath the machined surfaces.
- Depth of cut has no significant effect on the residual stress profiles or the surface topography.

4. Acknowledgements

This work is part of the project Turn2Flex (*Vinnova 2021-01274*) financed by the Swedish government agency for Enterprise and Innovation. Special thanks to AB SKF, Sumitomo Hartmetall Electric GmbH, and Ovako AB for support of material and manufacturing of samples. Thanks to Dr. Yiming Yao for support with the SEM analysis. We also thank Thord Johansson and Dr. Thomas Björk for the valuable discussion and support.

References

[1] Nabil Jouini, Philippe Revel, Guillaume Thoquenne. Influence of surface integrity on fatigue life of bearing rings finished by precision hard turning and grinding. J. Manuf. Proc. 2020;57:444-451

[2] Wisley F. Sales, Julius Schoop, Leonardo R.R. da Silva, Álisson R. Machado, I.S. Jawahir. A review of surface integrity in machining of hardened steels. J. Manuf. Proc. 2020;58:136:162

[3] S.B. Hosseini, K. Ryttberg, J. Kaminski, U. Klement. Characterization of the Surface Integrity Induced by Hard Turning of Bainitic and Martensitic AISI 52100 Steel. Procedia CIRP. 2012;1:494-499

[4] Werner Ankener, Marek Smaga, Julian Uebel, Jörg Seewig, Felix Grossmann, Stephan Basten, Benjamin Kirsch, Jan C. Aurich, Tilmann Beck. Depth-resolved characterization of cryogenic hard turned surface layer of AISI 52100 by X-ray diffraction and scanning electron microscopy investigations. Procedia CIRP. 2022;108:66-71

[5] J. D. Thiele and S. N. Melkote. Effect of tool edge geometry on workpiece subsurface deformation and through-thickness residual stresses for hard turning of AISI 52100 steel. Journal of Manufacturing Processes 2000; 2(4):270–276.

[6] Pawar S, Salve A, Chinchanikar S, Kulkarni A, Lamdhade G. Residual stresses during hard turning of AISI 52100 steel: numerical modelling with experimental validation. Mater Today Proc 2017;4:2350–9.

[7] E. Capello, P. Davoli, G. Bassanini, A. Bisi. Residual stresses and surface roughness in turning. J. Eng. Mater. Technol. 1991;121:346-351.

[8] W. Jomaa, V. Songmene, P. Bocher.An investigation of machining-induced residual stresses and microstructure of induction-hardened AISI 4340 steel. Mater. Manuf. Process 2016;31:838-844.

[9] P. Revel, N. Jouini, G. Thoquenne, F. Lefebvre. High precision hard turning of AISI 52100 bearing steel. Precis Eng. 2016;43:24-33.

[10] Weiwei Zhang, Kejia Zhuang. Effect of cutting edge microgeometry on surface roughness and white layer in turning AISI 52100 steel. Procedia CIRP 2020; 87:53-58.

[11] A Mittal, M Mehta. Surface finish prediction models for fine turning. Int. J. Prod. Res.1988:26 (12):1861–1876

[12] W Grzesik. A revised model for predicting surface roughness in turning. Wear 1996: 194:143-148.

[13] Stead J. Micro-metallography and its practical application. Journal of Western Scottish Iron and Steel Institute 1912;19:169–204.

[14] Hosseini, S.B., Klement, U. A descriptive phenomenological model for white layer formation in hard turning of AISI 52100 bearing steel. CIRP J. Manuf. Sci. Technol. 2021;32:299–310.

[15] Philippe Revel, Nabil Jouini, Guillaume Thoquenne, Fabien Lefebvre. High precision hard turning of AISI 52100 bearing steel. Precision Engineering 2016;43:24-33.

[16] Patrik Dahlman, Fredrik Gunnberg, Michael Jacobson. The influence of rake angle, cutting feed and cutting depth on residual stresses in hardturning. Journal of Materials Processing Technology 2004;147:181 184.

[17] P.I. Varela, C.S. Rakurty, A.K. Balaji. Surface Integrity in Hard Machining of 300M Steel: Effect of Cutting-edge Geometry on Machining Induced Residual Stresses. Procedia CIRP 2014;13:288-293.

[18] S.B. Hosseini, U. Klement, Y.Yao, K. Ryttberg. Formation mechanisms of white layers induced by hard turning of AISI 52100 steel. Acta materialia 2015;89:258-267.

[19] S.B. Hosseini, T. Beno, U. Klement, J. Kaminski, K. Ryttberg. Cutting temperatures during hard turning—Measurements and effects on white layer formation in AISI 52100. Journal of Materials Processing Technology (2014);214(6):1293-1300.

[20] Smith,S., Melkote, S.N., Lara-Curzio, E Watkins, T.R., Allard, l., Riester,L. Effect of surface integrity of hard turned AISI 52100 Steel on Fatigue performance. Materials Science and Engineering A, 459:333 -346.

[21] Bicek M, Dumont F, Courbon C, Pusavec F, rech J, Kopac J. Cryogenic machining as an alternative turning process of normalized and hardened AISI 52100 bearing steel. J Mater Process Technology. 2012; 21 2; 2609:18.